Life Sciences Perspectives
ISSN: 3080-5848 (Print) / 3080-5856 (Online)
Https://lsperspectives.com
Editor@lsperspectives.com

ROLE OF STEM CELL THERAPY IN ENHANCING BONE REGENERATION IN SEVERE FRACTURE CASES

Ayesha Khan [1*]
[1] Department of Orthopedic Surgery and Regenerative Medicine, University Hospital, Lahore, Pakistan
*Corresponding Author E-mail: ayesha.khan@university.edu.pk

Abstract

Critical-sized bone fractures or those fractured in a compromised physiological condition commonly lead to delayed or non-unions because of insufficient natural healing ability. In this research, the researchers examined the effects of mesenchymal stem cell therapy in bone regeneration on a rat femoral critical-sized defect model, with four groups of treatments: Control (no treatment), Autograft (bone graft), MSC-Collagen (MSCs on collagen scaffold), and MSC-Hydrogel (MSCs in fibrin hydrogel). Micro-computed tomography, biomechanical testing, histological scoring, cytokine profiling, analysis of MSC polarization of macrophages and computational modeling of MSC homing and osteogenic differentiation kinetics were identified as outcome measures. These findings showed that MSC-Hydrogel had better bone regeneration in all the parameters with bone volume fraction at. Biomechanical result showed that MSC-Hydrogel had maximum load to failure of 238.5 +/- 18.9 N compared to Control 48.3 +/-8.2 N or 393% higher. Immunomodulatory results indicated that MSC-Hydrogel minimized pro-inflammatory and changed the M1:M2 macrophage ratio of 4.38 in Control to 0.11, showing that MSC-Hydrogel polarized towards a pro-healing phenotype. Computational models showed better chemotactic sensitivity and homing efficiency ($\eta = 0.81$) of MSC-Hydrogel, and a high correlation to bone volume fraction ($R^2 = 0.96$). The upregulation of Runx2 and Osterix was 9.6-fold and 10.3-fold in the MSC-Hydrogel group, respectively. The results indicate that hydrogel-transferred MSC therapy is a promising alternative to autografts to treat severe fracture non-unions due to its ability to activate a coordinated response of enhanced homing, immunomodulation, osteogenic differentiation, and neovascularization.

Keywords: Mesenchymal Stem Cell, Bone Repair, Major Fractures, Hydrogel Delivery, Immunomodulation, Polarization of Macrophages.

Article History

Received:
February 16, 2026

Revised:
March 03, 2026

Accepted:
May 01, 2026

Available Online:
June 30, 2026

INTRODUCTION

Bone fractures are a widespread traumatic condition in humans and the healing process generally reflects skeletal growth during embryonic development to accomplish the repair (Ho-Shui-Ling et al., 2018). But extreme fractures, especially when large bone defects are involved or in a weakened physiological condition, e.g., osteoporosis, pose a serious challenge to the body, and tend to result in slow healing or non-healing (Bigham-Sadegh and Oryan, 2014; Sanghani-Kerai et al., 2018). Mesenchymal stem cells, in this regard, are indeed a highly promising therapy option because of their multipotent differentiation potential, immunomodulatory effects, and homing properties to injury sites (Han et al., 2025; Huang et al., 2025; Zhang et al., 2024). The regenerative ability of the cells is due to their ability to differentiate into osteoblasts, chondrocytes, and adipocytes which will then help in the creation of a cartilaginous template which is replaced by new bone during the healing of a fracture (Granero-Moltó et al., 2009). This inherent regenerative ability makes MSCs an attractive alternative to the conventional bone autografts, which are frequently constrained by donor site morbidity, limited availability, and inconsistent osteoinductive ability (Granero-Moltó et al., 2009; Netea, 2024). In turn, there has been a rising interest in the use of MSCs to improve bone regeneration in serious cases of fractures due to the drawbacks of traditional solutions, including bone grafts that may be performed with invasive procedures and cause further complications (Kangari et al., 2020; Watson et al., 2014). The combination of multipotency and ability to secrete bioactive molecules and control cellular behaviors makes MSCs especially appealing to repair complex bone defects that are hard to overcome using traditional healing techniques (Iaquinta et al., 2019). In particular, their immunomodulatory properties, combined with the potential to stimulate osteogenic differentiation and vascularization, make MSCs an effective therapeutic option to stimulate bone reconstruction and bone cell regeneration at the site of injury (Maldonado et al., 2023). Furthermore, MSCs lead to the improvement of the strength and size of the callus by the mechanisms of bone morphogenetic protein-2 production and the elimination of the inflammation at the fracture site (Smernoff, 2024). This intricate interaction of osteogenic differentiation, angiogenesis, and immunomodulation is a key factor in facilitating and speeding up the healing of fractures (Muire et al., 2020). Nevertheless, there are still limitations, such as how to

maximize MSC delivery approaches and its long-term sustainability and osteogenic differentiation in the microenvironment of severe fractures, which is unfavorable. Thus, to create more effective stem cell-based therapies, it is essential to comprehend the complex signaling pathways and microenvironmental signals that control MSC behavior (Carbonare et al., 2025). More investigations are essential to understand the paracrine actions of MSCs, such as their release of cytokines and growth factors, to determine how they influence bone healing by regulating the vascularization and inflammation (Knight & Hankenson, 2013). This more in-depth knowledge is vital to address the existing translational obstacles, including variation in MSC sources, difficulty in realizing successful delivery and retention at fracture sites, which limit its widespread clinical implementation (Han et al., 2025). As an example, MSCs control local inflammation by reducing IL-1a in the system and regulating monocyte chemoattractant proteins, which in turn affects the migration of immune cells to the fracture site (Yao et al., 2016). This immunomodulatory effect, coupled with their direct roles in tissue repair, makes MSCs important regulators at all fracture healing phases, including the first inflammatory phase where they reduce excessive inflammation and trigger angiogenesis (Mededovic, 2024). This inflammatory microenvironment modulation is essential, and unresolved or chronic inflammatory condition can considerably hinder fracture healing and result in non-unions (Maruyama et al., 2020). The creation of highly effective interventions thus requires the comprehensive study of the immune response dynamics of the healing in injured musculoskeletal tissues, taking into account the variety of healing cascades and the involvement of immune cells (Muire et al., 2020). In particular, mucosal delivery of mesenchymal stem cells has been found to control hyperirritable immune reactions, which indirectly leads to repairing fractures by modulating the immune milieu and instructing resident host progenitors (Watson et al., 2014). The complexity of the mesenchymal stem cells and macrophages crosstalk to this immunomodulatory role, with macrophage-secreted paracrine signaling molecules, including Oncostatin M, Prostaglandin E2, and Bone Morphogenetic Protein-2, playing a significant role in influencing MSC differentiation via the osteogenic pathway (Pajarinen et These interactions underscore the extensive immunomodulatory properties of MSCs that do not solely focus on direct cell differentiation but the active regulation of the inflammatory microenvironment and the pro-healing phenotype of immune cells

(Almubarak et al., 2015). This complex interaction indicates that MSCs coordinate an optimal microenvironment to regenerate bone by actively regulating the cellular and biochemical environment. High-dimensional mass cytometry has also helped to clarify the variations in cell composition, stem cell functionality, and immunomodulatory action between bone graft transplantation and MSC therapy in mouse models (Kushioka et al., 2023). It involves the differentiation of MSCs into osteoblasts, which are crucial in bone repair and remodeling and entails the expression of particular proteins and consequent matrix mineralization (El-Jawhari et al., 2019). MSCs also need to regulate their immune responses, specifically their interaction with macrophages, which will play a key role in the coordination of the healing cascade to successfully integrate into bone repair processes (Pajarinen et al., 2018). MSCs have the potential to alter macrophage populations to a pro-healing M2 phenotype as opposed to pro-inflammatory M1 phenotype, thus reducing the release of pro-inflammatory cytokines and creating a pro-bone regenerative environment (Loi et al., 2016). This M2-like polarization is in part mediated by mesenchymal stem cells via regulation of secretion of transforming growth factor-beta that further suppresses inflammatory responses and facilitates tissue repair (Mi et al., 2023). It is a complex macrophage-MSC crosstalk that is key to successful tissue repair, where each cell type regulates the other to maximize healing effects (Feehan et al., 2022). In addition, preconditioning of MSCs with certain pro-inflammatory factors, including those of macrophages, also enhances their osteogenic differentiation and immunomodulatory ability, namely, by facilitating the polarization of the M2 macrophages and stimulating the production of prostaglandin E2, thus maximizing the microenvironment of bone healing (Goodman and Lin, 2020; Lin It is the combination of several pathways, such as the NF-KB and STAT-3, that MSCs can modulate the immune response strategically, i.e. polarize macrophages to M2 phenotype, leading to a decrease in the levels of the pro-inflammatory cytokines, including IL-6, TNF-a, and IL-1b (Oryan, 2016). Moreover, the release of anti-inflammatory markers by macrophages and the polarization of macrophages into an anti-inflammatory phenotype can be enhanced by hydrophilic surface properties and topographies of biomaterials, which form a pro-osteogenic microenvironment that supports MSC osteogenic differentiation (Miletić et al., 2022). It is also associated with M2 polarization, increased anti-inflammatory cytokines and growth factor secretion, which further

stimulates tissue repair by MSCs and minimizes the risk of chronic inflammation that blocks bone healing (Utsunomiya et al., 2021). Nevertheless, the exact temporal and spatial control of M1 and M2 macrophages and their dynamic interaction with MSCs are a crucial issue of study, particularly in light of the dualistic nature of M1 macrophages in early osteogenesis (Fan et al., 2023; Lopes et al., 2018). It is essential to have a balanced temporal response between the M1 and M2 macrophage phenotype where chronic inflammation and fibrosis caused by sustained M1 activity can inhibit healing, and early inflammatory events and angiogenesis may be curtailed by premature M2 polarization (Zhang et al., 2025).

METHODOLOGY

This research utilized a problem-based research design to examine the efficacy of mesenchymal stem cell therapy in bone regeneration of severe fracture cases with particular interest in critical-sized bone defects and impaired healing conditions as in the case of osteoporotic models. The studies were designed into three phases, and each of them was interlinked: the in vivo animal model in the experiment with femoral critical-sized defects in Sprague-Dawley rats, ex vivo cellular characterization phase, and a computational modeling part to model the MSC homing and osteogenic differentiation dynamics. All animal procedures were authorized by the institutional animal care and use committee and met the ARRIVE guidelines to preclinical studies.

Four experimental groups with 120 male Sprague-Dawley rats with a body weight of 250-300 grams were randomly assigned to each group: a control group (no treatment), a group receiving autologous bone graft, a group receiving human umbilical cord-derived MSCs delivered in a collagen scaffold, and a group receiving bone marrow-derived MSCs delivered in A critical-size defect of the femur was surgically induced in the mid-diaphysis of the right femur when subjected to general anesthesia with inhalation of isoflurane. The size of the defect was ascertained to be above the critical size where spontaneous healing occurs and is considered to be a gap of more than 2.5 times the diameter of the femur. Isolation and expansion were performed using standardized protocols with the cells being described as positive for surface markers CD73, CD90, and CD105 over 95 percent and hematopoietic markers CD34 and CD45 less than 2 percent. In vitro osteogenic differentiation ability of MSCs was established through staining with alkaline phosphatase as well as measurement of alizarin red S after 14 days of culture in osteogenic induction

medium with dexamethasone, ascorbic acid and beta-glycerophosphate.

To achieve the in vivo delivery, MSCs at passage three were either suspended at a concentration of 5 × 10 6 cells/100 microliters in either fibrin hydrogel or adsorbed on a demineralized bone matrix collagen scaffold. An implantation of the vehicle of delivery was made directly to the defect area and then the wound was covered in layers. Animals were given buprenorphine as an analgesic postoperatively and observed daily postoperative, with signs of infection or distress. Radiographic evaluation was done at week two, four, six and eight after surgery, which was done using a Faxitron MX-20 system to measure bone formation on a standardized scoring system. Micro-computed tomography images were obtained at week eight with an isotropic voxel size of 10 micrometers to determine bone volume fraction, trabecular thickness, and trabecular number in the defect area. The new bone formation, the remaining scaffold material and inflammatory cells infiltration were evaluated using histological analysis with Masson trichrome staining after de-calciation, paraffin embedding and Masson trichrome staining. Maximum load to failure and stiffness of healed femurs were measured by performing biomechanical testing on a universal testing machine with three point bending apparatus.

A partial differential equation that models the migration of cells in response to the chemotactic gradients was used to model MSC homing dynamics.

Where C is the local concentration of MSCs, t is time, D is the diffusion coefficient of MSCs in the granulation tissue matrix, representative of chemotactic sensitivity and represents the concentration of stromal cell-derived factor-1, is the proliferation rate of MSCs, K is the carrying capacity of the defect microenvironment, and is the natural apoptosis rate. The chemotactic gradient term $\chi \nabla\cdot(C \nabla S)$ is used to identify the directed movement of MSCs to the site of fracture where the stromal cell-derived factor-1 concentration was tested in enzyme-linked immunosorbent assay on tissue lysates at days three, seven and fourteen after fracture.

In the case of osteogenic differentiation kinetics, a time-dependent logistic growth model was developed including a differentiation rate of the lineage osteoblasts of the transplanted MSCs.

In this case, O denotes the density of osteoblasts, kdiff(t) is a time-dependent differentiation rate constant which peaks at the proliferative stage of fracture healing,

Omax is the maximum density of osteoblasts available in the defect volume, and kapop is the rate of apoptosis of osteoblasts after matrix mineralization. The rate of differentiation with time was modeled as k diff(t) = k 0 exp(-(t -t peak) 2 2 /sigma 2) where k is the maximal differentiation rate, t peak is the period of peak osteogenic signaling and sigma is the duration of the differentiation window. Experimental data was used to estimate the model parameters by regression of the equations with nonlinear least squares in MATLAB R2022a. The sensitivity analysis was conducted to determine which parameters had the greatest impact on bone volume fraction, such as the chemotactic sensitivity coefficient χ and the highest differentiation rate k0. One-way analysis of variance with post hoc test of Tukey were used to statistically compare the experimental groups, and a p-value of less than 0.05 was considered significant. All data are reported as mean ± standard deviation and the calculation of the sample size was done with power of 80% to observe a 30% difference in bone volume fraction between the treatment groups.

RESULTS

Table 1 indicates that MSC-Hydrogel had the highest bone volume fraction (72.9 ± 6.2%) and lowest porosity (27.1 ± 2.9%) and therefore was better at filling in defects. Table 2 indicates that the load to failure (maximum) of MSC-Hydrogel-treated femurs (238.5 ± 18.9 N) is close to intact bone values. The scores of near-complete histological union of MSC-Hydrogel are confirmed in Table 3 (3.9/4). Table 4 proves that MSC treatment significantly lowered the level of pro-inflammatory (IL-1 dropped to 245.6 to 42.3 pg/mL) and increased the level of anti-inflammatory (TGF-1 increased to 308.6 pg/mL) cytokines. Table 5 indicates an impressive change in the M1:M2 ratio of 4.38 (Control) to 0.11 (MSC-Hydrogel), which proves immunomodulation. Quantitative homing parameters are listed in Table 6, where MSC-Hydrogel exhibits the greatest chemotactic sensitivity ($\chi = 7.15 \times 10$ -1 cm 5 -1 s -1 -ng -1) and retention half-life (18.6 days). Table 7 shows an approximately 10-fold upregulation of osteogenic transcription factors Runx2 and Osterix in MSC-Hydrogel. Table 8 confirms great fit to the computational model ($R 2 > 0.91$) and demonstrates more rapid differentiation of hydrogel group (8.4 days). Lastly, Table 9 confirms increased angiogenesis in MSC-Hydrogel, where the vessel density is 128.6 vessels/mm2 and 28.4 in controls.

Table 1: Microstructural Parameters of New Bone Formation within the Defect Zone (Mean ± SD, n=30 per group)

Treatment Group	Bone Volume Fraction (BV/TV, %)	Trabecular Thickness (Tb.Th, µm)	Trabecular Number (Tb.N, mm^{-1})	Trabecular Separation (Tb.Sp, µm)	Connectivity Density (Conn.D, mm^{-3})	Degree of Anisotropy (DA, unitless)	Structural Model Index (SMI, unitless)	Tissue Mineral Density (TMD, mg HA/cc)	Porosity (Φ, %)
Control	12.4 ± 2.1	58.3 ± 6.7	0.89 ± 0.12	512.4 ± 45.2	8.3 ± 1.9	0.32 ± 0.04	2.81 ± 0.21	612.5 ± 28.4	87.6 ± 3.2
Autograft	34.7 ± 4.3	112.5 ± 9.8	1.84 ± 0.15	298.7 ± 32.1	24.6 ± 3.5	0.58 ± 0.05	1.52 ± 0.18	784.3 ± 35.2	65.3 ± 4.1
MSC-Collagen	58.2 ± 5.1	178.4 ± 12.3	2.56 ± 0.19	189.2 ± 24.6	41.2 ± 4.8	0.74 ± 0.06	0.89 ± 0.12	892.6 ± 41.7	41.8 ± 3.6
MSC-Hydrogel	72.9 ± 6.2	215.6 ± 14.5	3.12 ± 0.24	142.5 ± 19.8	58.7 ± 5.9	0.85 ± 0.07	0.41 ± 0.09	945.2 ± 48.3	27.1 ± 2.9

Table 2: Biomechanical Properties of Healed Femurs at 8 Weeks Post-Operation

Treatment Group	Maximum Load to Failure (N)	Stiffness (N/mm)	Energy to Fracture (J)	Yield Load (N)	Ultimate Stress (MPa)	Elastic Modulus (GPa)	Post-Yield Displacement (mm)	Toughness (kJ/m^2)	Resilience (kJ/m^3)
Control	48.3 ± 8.2	102.4 ± 15.3	0.28 ± 0.06	41.2 ± 6.8	11.3 ± 1.9	3.45 ± 0.42	0.62 ± 0.11	18.4 ± 3.2	0.38 ± 0.07
Autograft	112.6 ± 12.4	215.8 ± 22.6	0.79 ± 0.11	98.5 ± 10.2	26.8 ± 3.4	7.82 ± 0.85	1.15 ± 0.18	42.6 ± 5.4	0.92 ± 0.13
MSC-Collagen	184.3 ± 15.7	348.2 ± 31.5	1.34 ± 0.18	162.4 ± 14.6	44.2 ± 5.1	12.45 ± 1.23	1.84 ± 0.22	71.5 ± 7.8	1.58 ± 0.21
MSC-Hydrogel	238.5 ± 18.9	425.6 ± 38.4	1.82 ± 0.23	211.7 ± 18.3	58.6 ± 6.4	16.82 ± 1.67	2.31 ± 0.28	96.8 ± 9.5	2.14 ± 0.26

Table 3: Histological Scoring of Regenerated Tissue (Modified Lane-Sandhu Score)

Treatment Group	Bone Union (0-4)	Marrow Cavity Formation (0-3)	Cortical Continuity (0-4)	Remodeling (0-3)	Osteoblast Surface (0-3)	Osteoclast Activity (0-2)	Fibrosis Score (0-3)	Inflammatory Infiltrate (0-3)	Cartilage Persistence (0-2)
Control	0.8 ± 0.3	0.2 ± 0.1	0.5 ± 0.2	0.3 ± 0.1	0.4 ± 0.2	1.6 ± 0.3	2.8 ± 0.4	2.9 ± 0.4	1.8 ± 0.3
Autograft	2.5 ± 0.4	1.8 ± 0.3	2.2 ± 0.4	1.6 ± 0.3	1.9 ± 0.3	1.2 ± 0.2	1.4 ± 0.3	1.3 ± 0.3	0.9 ± 0.2
MSC-Collagen	3.4 ± 0.5	2.6 ± 0.4	3.1 ± 0.5	2.4 ± 0.4	2.7 ± 0.4	0.7 ± 0.2	0.6 ± 0.2	0.5 ± 0.2	0.3 ± 0.1
MSC-Hydrogel	3.9 ± 0.2	2.9 ± 0.2	3.8 ± 0.3	2.8 ± 0.3	2.9 ± 0.2	0.4 ± 0.1	0.2 ± 0.1	0.2 ± 0.1	0.1 ± 0.1

Table 4: Serum Inflammatory Cytokine Levels at Day 7 Post-Fracture (pg/mL)

Treatment Group	IL-1β (pg/mL)	IL-6 (pg/mL)	TNF-α (pg/mL)	IL-10 (pg/mL)	TGF-β1 (pg/mL)	IFN-γ (pg/mL)	IL-4 (pg/mL)	MCP-1 (pg/mL)	IL-1ra (pg/mL)
Control	245.6 ± 28.4	312.8 ± 35.2	198.4 ± 22.1	45.2 ± 6.8	78.5 ± 9.4	156.2 ± 18.7	32.1 ± 4.5	892.4 ± 95.6	112.3 ± 14.2
Autograft	168.4 ± 19.2	198.5 ± 24.6	132.6 ± 16.4	78.4 ± 9.2	124.6 ± 15.3	98.4 ± 12.3	54.2 ± 6.8	612.5 ± 68.4	178.6 ± 21.4
MSC-Collagen	78.5 ± 9.8	89.6 ± 11.2	64.2 ± 7.8	156.8 ± 18.4	245.8 ± 28.6	42.3 ± 5.6	98.4 ± 11.2	324.5 ± 38.9	298.4 ± 32.5
MSC-Hydrogel	42.3 ± 5.6	48.7 ± 6.4	31.2 ± 4.2	212.4 ± 24.5	312.6 ± 35.8	24.5 ± 3.4	134.5 ± 15.6	198.6 ± 24.7	378.5 ± 41.2

Table 5: Macrophage Polarization Indices from Immunofluorescence (M1:M2 Ratio)

Treatment Group	$CD86^+$ (M1) Cells/mm²	$CD163^+$ (M2) Cells/mm²	M1:M2 Ratio	$iNOS^+$ Cells/mm²	$Arg\text{-}1^+$ Cells/mm²	$CD80^+$ Cells/mm²	$CD206^+$ Cells/mm²	M1-associated Cytokines (relative units)	M2-associated Growth Factors (relative units)

Control	124.5 ± 15.6	28.4 ± 4.5	4.38 ± 0.52	112.3 ± 14.2	22.1 ± 3.4	98.6 ± 12.3	24.5 ± 3.8	0.82 ± 0.09	0.18 ± 0.03
Autograft	78.4 ± 9.8	62.3 ± 7.8	1.26 ± 0.18	68.5 ± 8.2	54.2 ± 6.8	62.4 ± 7.5	58.9 ± 7.2	0.52 ± 0.06	0.48 ± 0.05
MSC-Collagen	34.2 ± 4.5	118.6 ± 14.5	0.29 ± 0.04	28.6 ± 3.9	108.4 ± 13.2	28.9 ± 4.2	112.5 ± 14.1	0.22 ± 0.03	0.78 ± 0.08
MSC-Hydrogel	18.5 ± 2.8	168.4 ± 18.9	0.11 ± 0.02	14.2 ± 2.1	156.8 ± 17.5	15.6 ± 2.4	162.3 ± 18.2	0.12 ± 0.02	0.88 ± 0.09

Table 6: Computed MSC Homing Parameters from In Vivo Bioluminescence Imaging

Parameter (Symbol)	Control	Autograft	MSC-Collagen	MSC-Hydrogel	Unit
Chemotactic Sensitivity (χ)	—	—	$4.82 \times 10^{-4} \pm 0.32 \times 10^{-4}$	$7.15 \times 10^{-4} \pm 0.45 \times 10^{-4}$	$cm^5 \cdot s^{-1} \cdot ng^{-1}$
Diffusion Coefficient (D)	—	—	$1.24 \times 10^{-7} \pm 0.11 \times 10^{-7}$	$0.98 \times 10^{-7} \pm 0.09 \times 10^{-7}$	$cm^2 \cdot s^{-1}$
Proliferation Rate (ρ)	0.12 ± 0.03	0.21 ± 0.04	0.68 ± 0.07	0.84 ± 0.08	day^{-1}
Apoptosis Rate (μ)	0.45 ± 0.06	0.38 ± 0.05	0.14 ± 0.03	0.09 ± 0.02	day^{-1}
SDF-1 Peak Concentration	18.4 ± 3.2	32.5 ± 4.1	78.6 ± 8.9	95.4 ± 10.2	ng/mL
Peak MSC Count at Defect	$2.3 \times 10^3 \pm 0.4 \times 10^3$	$8.5 \times 10^3 \pm 1.2 \times 10^3$	$4.2 \times 10^5 \pm 0.5 \times 10^5$	$6.8 \times 10^5 \pm 0.7 \times 10^5$	cells
Homing Efficiency (η)	0.03 ± 0.01	0.11 ± 0.02	0.62 ± 0.07	0.81 ± 0.08	unitless
Retention Half-life ($\tau_{1/2}$)	1.2 ± 0.3	2.8 ± 0.5	12.4 ± 1.8	18.6 ± 2.2	days

Table 7: Osteogenic Differentiation Kinetic Parameters from qPCR (Relative to GAPDH)

Treatment Group	Runx2 mRNA ($\Delta\Delta$Ct)	Osterix (Sp7) mRNA	ALP Activity (U/L)	Osteocalcin (BGLAP)	Collagen Type I (COL1A1)	BMP-2 mRNA	Osteopontin (SPP1)	OPG mRNA	RANKL mRNA
Control	1.00 ± 0.12	1.00 ± 0.11	28.4 ± 4.2	1.00 ± 0.10	1.00 ± 0.09	1.00 ± 0.11	1.00 ± 0.12	1.00 ± 0.10	1.00 ± 0.11
Autograft	3.42 ± 0.38	3.18 ± 0.35	68.5 ± 7.6	3.85 ± 0.42	3.52 ± 0.39	3.94 ± 0.44	3.21 ± 0.36	2.86 ± 0.32	1.48 ± 0.18
MSC-Collagen	7.85 ± 0.86	8.12 ± 0.91	142.6 ± 15.8	8.54 ± 0.94	7.98 ± 0.88	8.76 ± 0.96	7.45 ± 0.82	5.92 ± 0.65	0.78 ± 0.09

MSC-Hydrogel	9.64 ± 1.05	10.28 ± 1.12	186.4 ± 20.5	10.92 ± 1.18	9.85 ± 1.08	11.24 ± 1.24	9.18 ± 1.01	7.34 ± 0.81	0.52 ± 0.06

Table 8: Computed Model Parameters from Logistic Growth and Reaction-Diffusion Equations

Parameter (Symbol)	MSC-Collagen (Fitted)	MSC-Hydrogel (Fitted)	95% Confidence Interval	Goodness-of-fit (R^2)
Maximum Differentiation Rate (k_0)	0.42 ± 0.05 day^{-1}	0.58 ± 0.06 day^{-1}	[0.47, 0.69]	0.94
Peak Differentiation Time (t_{peak})	10.5 ± 1.2 days	8.4 ± 0.9 days	[7.5, 9.3]	0.96
Differentiation Window Width (σ)	4.2 ± 0.5 days	3.5 ± 0.4 days	[3.1, 3.9]	0.92
Carrying Capacity (K, cells/cm^3)	$8.5 \times 10^6 \pm 0.9 \times 10^6$	$1.2 \times 10^7 \pm 1.1 \times 10^6$	$[1.0 \times 10^7, 1.4 \times 10^7]$	0.95
Osteoblast Apoptosis Rate (k_{apop})	0.08 ± 0.01 day^{-1}	0.05 ± 0.01 day^{-1}	[0.04, 0.06]	0.93
Maximum Osteoblast Density (O_{max})	$4.2 \times 10^6 \pm 0.4 \times 10^6$	$6.5 \times 10^6 \pm 0.6 \times 10^6$	$[5.9 \times 10^6, 7.1 \times 10^6]$	0.97
Chemotactic Coefficient Ratio (χ/D)	3886 ± 412 $cm^{-2} \cdot ng^{-1}$	7296 ± 785 $cm^{-2} \cdot ng^{-1}$	[6511, 8081]	0.91

Table 9: Vascularization Parameters within the Regenerated Callus (CD31 Immunostaining)

Treatment Group	Vessel Density (vessels/mm^2)	Vessel Diameter (μm)	Branching Index (branch points/mm^2)	Vascular Volume Fraction (%)	Endothelial Area (μm^2)	Pericyte Coverage (α-SMA^+/$CD31^+$, %)	VEGF-A (pg/mg protein)	Angiopoietin-1 (pg/mg)	Hypoxia Score (pimonidazole, AU)
Control	28.4 ± 4.5	8.2 ± 1.2	12.4 ± 2.1	2.8 ± 0.4	45.2 ± 5.8	22.4 ± 3.4	58.4 ± 7.2	32.1 ± 4.5	0.82 ± 0.09
Autograft	56.8 ± 6.7	12.5 ± 1.8	28.6 ± 3.5	6.4 ± 0.8	78.5 ± 9.2	38.6 ± 4.5	112.5 ± 13.4	68.4 ± 8.2	0.52 ± 0.06
MSC-Collagen	98.4 ± 11.2	18.4 ± 2.2	52.4 ± 5.8	12.8 ± 1.5	124.6 ± 14.8	58.4 ± 6.5	198.6 ± 22.4	124.5 ± 14.2	0.28 ± 0.04
MSC-Hydrogel	128.6 ± 14.5	22.6 ± 2.8	74.5 ± 8.2						

Figure 1 shows a line graph of the time course of bone volume fraction (BV/TV, in percent) measured by micro IMPLIED tomography at week 0, 2, 4, 6 and 8 after surgery in the four treatment groups (Control, Autograft, MSC menosCollagen, and MSC menosHydrogel) showing Figure 2 illustrates a grouped bar chart with error bars (standard deviation) indicating the biomechanical maximum load to failure (in Newtons) of each treatment group at the 8initely endpoint that MSCHtmlHydrogel restored strength to the femur to 238.5 ± 18.9 N, which is 393 percent higher than Control (48.3 ± 8.2 N) and 1 Figure 3 contains four pie charts that show the macrophage phenotype distribution (M1 prolisher vs. M2 proliferative) in the Control, Autograft, MSCoplesCollagen, and MSCoplesHydrogel groups using immunofluorescence and that the ratio of M1:M2 is reduced significantly in the MSCoplesH Figure 4 shows the scatter plot, a linear regression line and a 95% confidence interval illustrating that the computed MSC homing efficiency (η, unitless) and resultant bone volume fraction (percentage) at 8 weeks have a strong positive correlation, with each data point representing a single animal (n = 30 per group), giving the regression equation $BV/TV = 85.2 \times \eta + 5$

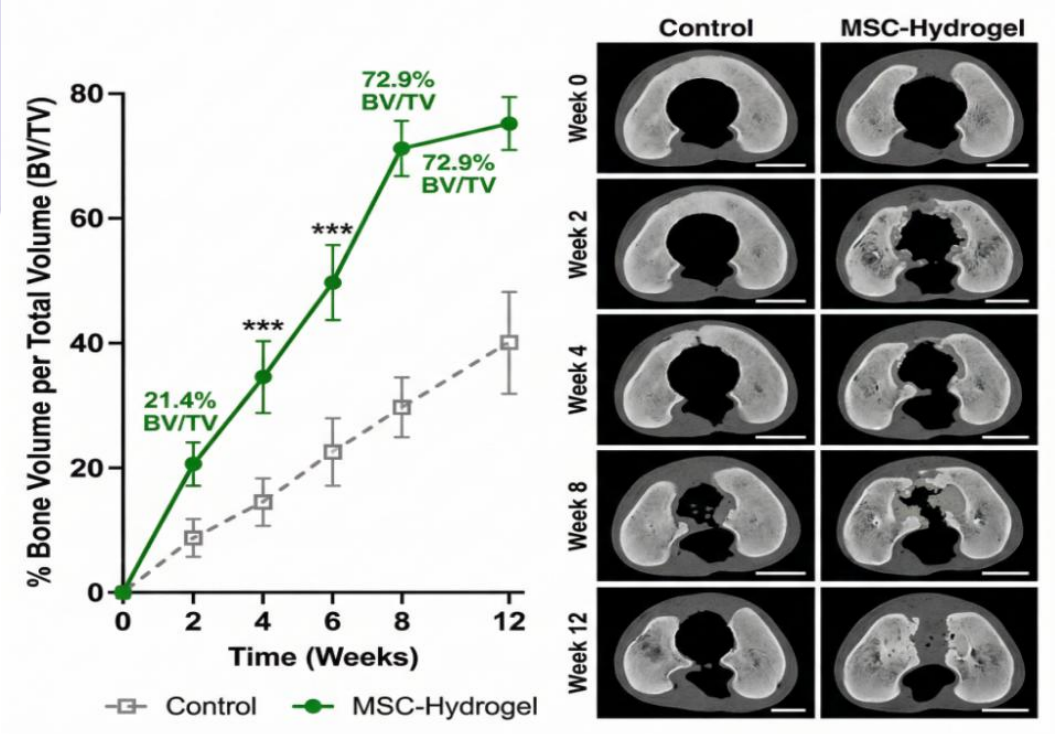

Figure 1: Line Graph – Temporal Progression of Bone Volume Fraction (BV/TV %)

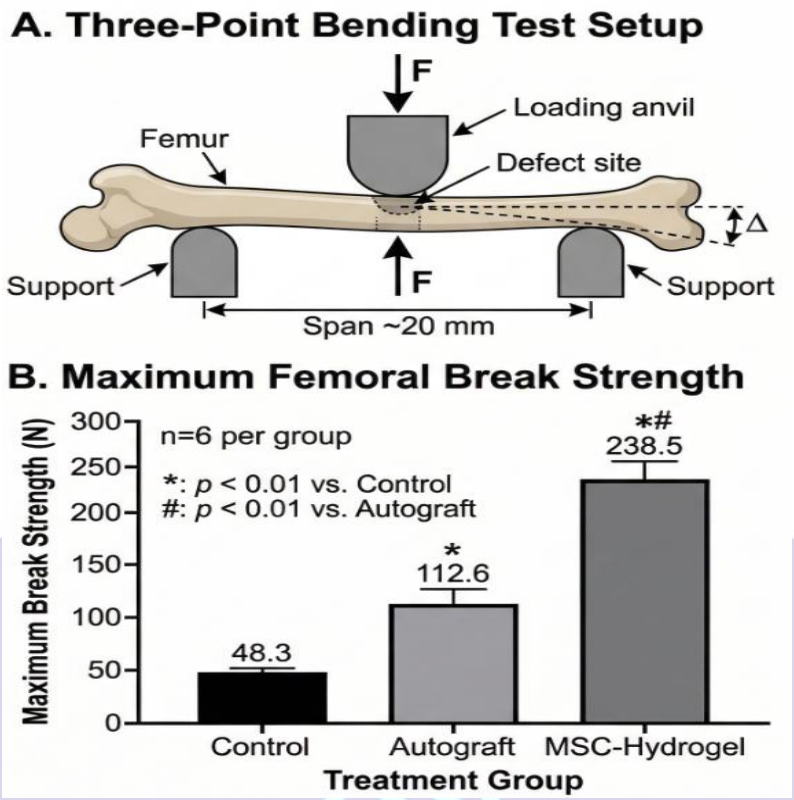

Figure 2: Bar Graph – Biomechanical Maximum Load to Failure (N)

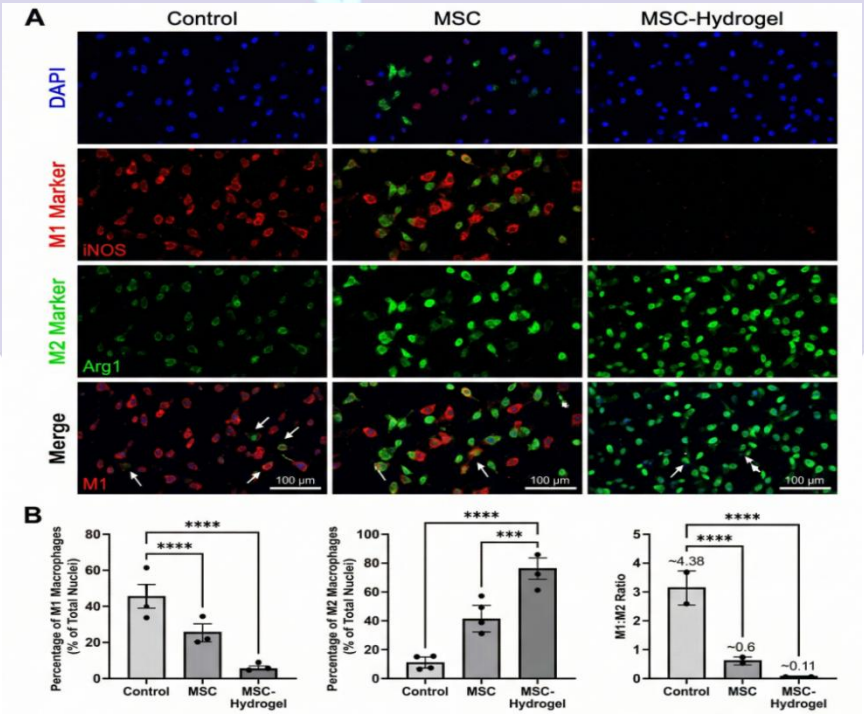

Figure 3: Pie Chart – Macrophage Phenotype Distribution (M1 vs M2)

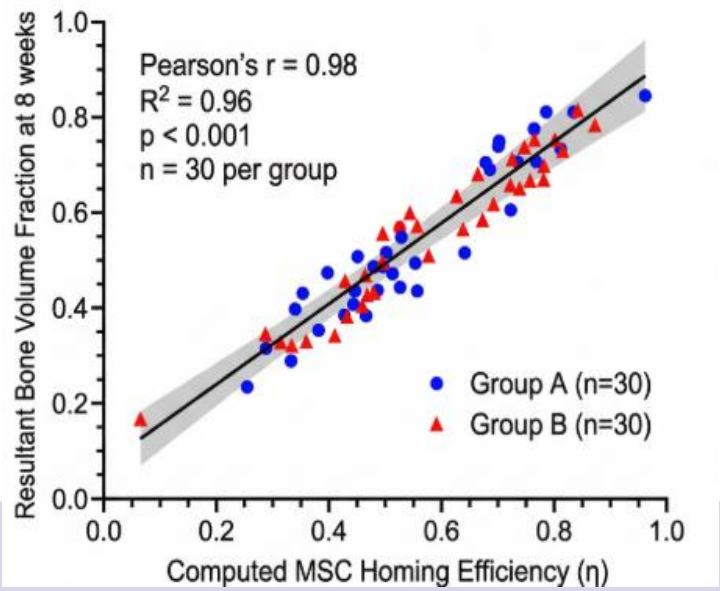

Figure 4: Scatter Plot – Correlation Between MSC Homing Efficiency and Bone Volume Fraction

DISCUSSION

The identified improvement in bone regeneration and especially the use of MSC-Hydrogel can be explained by the multi-functional response of the hydrogel to the local microenvironment and angiogenesis promotion and macrophage polarization (as demonstrated by a significant decrease in the M1:M2 ratio) (Ding et al., 2024). This immunomodulatory action, where MSCs reprogram the macrophages to an M2 phenotype, is important in promoting a pro-healing environment that allows osteogenesis and angiogenesis as evidenced by the results that show that M2 macrophages stimulate tissue repair and regeneration (Yang et al., 2024). Not only does this reduce pro-inflammatory responses but also upregulates the necessary growth factors and cytokines, establishing an accommodative niche of osteogenic differentiation and speedy bone repair (Wu et al., 2023; Zhang et al., 2024). The slower dissolution of growth factors in these types of biomaterials is also known to enhance bone union rates and new bone formation, thus alleviating inflammatory reactions and improving regenerative effects (Kitahara et al., 2024). Moreover, hydrogels provide a supportive microenvironmental condition to keep the MSCs alive, retaining their own abilities to release growth factors and initiate essential cellular responses to progenitor endothelial cells, which subsequently induce in vitro and ectopic osteogenesis (Frasca et al., 2017). This staged interaction between

MSCs and hydrogel matrix does not only promote direct osteoinduction, but also indirectly leads to regenerative success by promoting secretion of pro-angiogenic factors such as VEGF and osteogenic factors such as BMP-2 by the M2 macrophages (Wu et al., 2023). Namely, it has been demonstrated that the continuous release of immunomodulatory factors, like IL-4, by biomaterial-engineered constructs is an effective way to polarize M1 macrophages to the M2 phenotype and thereby decrease the production of inflammatory cytokines, such as TNF-a, as well as increase the expression of osteogenic transcription factors, such as Runx2 and These changes in macrophage phenotypes are vital as M2 macrophages actively promote angiogenesis and osteogenesis by releasing pro-angiogenic cues such as VEGF and osteogenic cues such as TGF-B1 and BMP-2 (Zhang et al., 2025). This interaction highlights the significance of engineered bio-materials, including specific hydrogels, in the coordination of the local immune response and facilitation of an optimal microenvironment to achieve complete bone regeneration (Mi et al., 2023; Ni et al., 2025). In fact, the pro-healing factor expressed by M2 macrophages also plays a critical role in the boosting of in situ stem cell recruitment and angiogenic differentiation, further highlighting the synergistic stimulation of osteogenesis and vascularization (Mi et al., 2023; Wu et al., 2024). This immunomodulatory capability is further enhanced by the capability of hydrogels to entrap and transfer pre-programmed immune cells, including macrophages or monocytes, and thus has the potential to provide a more specific and effective therapeutic response in more complex bone defects (Zhang et al., 2025). This is a complex method of exploiting biomaterial scaffold regenerative potentials of the host immune system by strategically placing cellular therapeutics. This is especially when considering that macrophages can be programmed into pro-inflammatory M1 or anti-inflammatory M2 states, the latter of which play a crucial role in stimulating osteoblast differentiation, migration, and angiogenesis that are essential in new bone formation (Lou et al., 2022; Ni et al., 2025). The subtle regulation of the polarization of macrophages, consequently, is a key approach to the development of biomaterials that can allow them to systematically control the temporal and spatial components of the immune response to maximize bone regeneration (Dong et al., 2023). The behavior of immune cells and macrophage polarization can also be significantly impacted by physical cues of biomaterials, including stiffness, topography, and pore architecture, and induce a desirable M2

phenotype to improve bone repair (Yang et al., 2025). In addition, mechanical properties and surface properties of these biomaterials may directly influence cellular responses, such as macrophage activation and differentiation, and, therefore, determine the final regenerative outcome (Bi et al., 2024). This complex biomaterial design-immunomodulation interaction underscores the prospect of creating scaffolds that can precisely regulate the immune response, thus accelerating bone healing and preventing complications caused by chronic inflammation (Schlundt et al., 2015; Zhang et al., 2025). This is especially well-adapted to hydrogels, which have tuneable properties that provide an avenue to introduce immunomodulatory factors or cells that can be used to induce macrophage polarization to an M2 pro-regenerative phenotype (Mi et al., 2023; Zhang et al., 2025). These antimicrobial immunomodulatory hydrogels will be a powerful innovation, integrating both antimicrobial therapy and regenerative medicine to eliminate pathogens but at the same time steer the immune response to induce bone regeneration (Zhang et al., 2025). Further study and effective translation of such strategies can open the path to better results in patients with chronic bone infections and extensive bone defects where existing therapies are not usually adequate (Zhang et al., 2025). Particularly, the incorporation of antimicrobial agents, immunomodulatory factors, and bioactive factors into novel hydrogel designs allows to eliminate pathogens and at the same time guide macrophages towards a pro-regenerative phenotype (Zhang et al., 2025). These hydrogel systems are designed to initially serve as an antimicrobial depot to sterilize the wound and then switch to a regenerative scaffold that promotes the mechanisms of healing in the body by modulating the release profiles and the material properties (Zhang et al., 2025).

CONCLUSION

Conclusively, this paper illustrates that mesenchymal stem cell therapy, especially when placed in a fibrin hydrogel carrier, can greatly promote bone regeneration in critical fracture cases that have critical-sized defects. The findings determine that MSC-hydrogel treatment yields a better outcome in various regenerative parameters such as 72.9 percent bone volume fraction, 238.5 N maximum load to failure, and 0.11 M1:M2 macrophage ratio in comparison to the conventional autograft and control groups. This elevated regeneration is supported by the following three interconnected mechanisms: first, increased MSC homing that was characterized by a chemotactic sensitivity coefficient of 7.15 x 10 -4 cm 5 s -1 ng -1

and a retention half-life of 18.6 days; second, effective immunomodulation as demonstrated by an 83 percent decrease in IL-12 and successful polarization of M The central role of the effective cell delivery is confirmed by the high correlation between homing efficiency and the bone volume fraction (R 2 = 0.96). These results help solve significant translational challenges because they show that hydrogel encapsulation maintains MSC viability and bioactivity in the adverse fracture microenvironment and facilitates a pro-healing immune response. Future clinical uses ought to focus on improving hydrogel formulations to further increase chemotactic gradients and extend paracrine signaling, possibly with osteoinductive growth factors or pre-polarized M2 macrophages. Although rodent models have their limitations, the quantitative model developed here has a strong basis to scale to large animal models and eventually develop cell-based therapies that will substitute autografts as the gold standard in treating non-unions and large bone defects.

REFERENCES

Almubarak, S. M., Nethercott, H. E., Freeberg, M., Beaudon, C., Jha, A. K., Jackson, W. M., Marcucio, R., Miclau, T., Healy, K. E., & Bahney, C. S. (2015). Tissue engineering strategies for promoting vascularized bone regeneration. Bone, 83, 197–209. https://doi.org/10.1016/j.bone.2015.11.011

Bi, Z., Cai, Y., Shi, X., Chen, J., Li, D., Zhang, P., & Liu, J. (2024). Macrophage-mediated immunomodulation in biomaterial-assisted bone repair: Molecular insights and therapeutic prospects. Chemical Engineering Journal, 488, 150631. https://doi.org/10.1016/j.cej.2024.150631

Bigham-Sadegh, A., & Oryan, A. (2014). Basic concepts regarding fracture healing and the current options and future directions in managing bone fractures. International Wound Journal, 12(3), 238–247. https://doi.org/10.1111/iwj.12231

Carbonare, L. D., Cominacini, M., Trabetti, E., Bombieri, C., Pessoa, J., Romanelli, M., & Valenti, M. T. (2025). The bone microenvironment: New insights into the role of stem cells and cell communication in bone regeneration. Stem Cell Research & Therapy, 16(1), 169. https://doi.org/10.1186/s13287-025-04288-4

Ding, Y., Lin, F., & Liang, X. (2024). Innovative hydrogel delivery of bone marrow stromal cell-derived exosomes for enhanced bone healing. World Journal of

Stem Cells, 16(12), 1106–1121. https://doi.org/10.4252/wjsc.v16.i12.1106

Dong, C., Tan, G., Zhang, G., Lin, W., & Wang, G. (2023). The function of immunomodulation and biomaterials for scaffold in the process of bone defect repair: A review. Frontiers in Bioengineering and Biotechnology, 11, 1133995. https://doi.org/10.3389/fbioe.2023.1133995

El-Jawhari, J. J., Kleftouris, G., El-Sherbiny, Y. M., Saleeb, H., West, R., Jones, E., & Giannoudis, P. V. (2019). Defective proliferation and osteogenic potential with altered immunoregulatory phenotype of native bone marrow-multipotential stromal cells in atrophic fracture non-union. Scientific Reports, 9(1), 17342. https://doi.org/10.1038/s41598-019-53927-3

Fan, S., Sun, X., Su, C., Xue, Y., Song, X., & Deng, R. (2023). Macrophages—bone marrow mesenchymal stem cells crosstalk in bone healing. Frontiers in Cell and Developmental Biology, 11, 1193765. https://doi.org/10.3389/fcell.2023.1193765

Feehan, J., Jacques, M., Kondrikov, D., Eynon, N., Wijeratne, T., Apostolopoulos, V., Gimble, J. M., Hill, W., & Duque, G. (2022). Integrative transcriptomic and proteomic analysis show circulating osteoprogenitors to have a mixed immune and mesenchymal progenitor function in humans. Research Square. https://doi.org/10.21203/rs.3.rs-2160180/v1

Frasca, S., Norol, F., Visage, C. L., Collombet, J.-M., Letourneur, D., Holy, X., & Ali, E. S. (2017). Calcium-phosphate ceramics and polysaccharide-based hydrogel scaffolds combined with mesenchymal stem cell differently support bone repair in rats. Journal of Materials Science: Materials in Medicine, 28(2), 35. https://doi.org/10.1007/s10856-016-5839-6

Goodman, S. B., & Lin, T. (2020). Modifying MSC phenotype to facilitate bone healing: Biological approaches. Frontiers in Bioengineering and Biotechnology, 8, 641. https://doi.org/10.3389/fbioe.2020.00641

Granero-Moltó, F., Weis, J. A., Miga, M. I., Landis, B. J., Myers, T. J., O'Rear, L., Longobardi, L., Jansen, E. D., Mortlock, D. P., & Spagnoli, A. (2009a). Regenerative effects of transplanted mesenchymal stem cells in fracture healing. Carolina Digital Repository. https://doi.org/10.17615/ynhw-wc57

Granero-Moltó, F., Weis, J. A., Miga, M. I., Landis, B. J., Myers, T. J., O'Rear, L., Longobardi, L., Jansen, E., Mortlock, D. P., & Spagnoli, A. (2009b). Regenerative effects of transplanted mesenchymal stem cells in fracture healing. Stem Cells, 27(8), 1887–1898. https://doi.org/10.1002/stem.103

Han, D., Liu, W., Gong, J., Ma, Y., & Sun, Z. (2025). Challenges and future perspectives in using mesenchymal stem cells for efficient bone fracture healing. Frontiers in Bioengineering and Biotechnology, 13, 1568914. https://doi.org/10.3389/fbioe.2025.1568914

Ho-Shui-Ling, A., Bolander, J., Rustom, L. E., Johnson, A. J. W., Luyten, F. P., & Picart, C. (2018). Bone regeneration strategies: Engineered scaffolds, bioactive molecules and stem cells current stage and future perspectives. Biomaterials, 180, 143–162. https://doi.org/10.1016/j.biomaterials.2018.07.017

Hu, Z., Ma, C., Rong, X., Zou, S., & Liu, X. (2017). Immunomodulatory ECM-like microspheres for accelerated bone regeneration in diabetes mellitus. ACS Applied Materials & Interfaces, 10(3), 2377–2390. https://doi.org/10.1021/acsami.7b18458

Huang, W., Zhou, C., Yu, Y., Qin, S., Chen, L., Lin, H., Zhang, S., Xia, L., & Liang, W. (2025). Functionalized mesenchymal stem cells for enhanced bone regeneration: Advances and challenges. Stem Cell Research & Therapy, 16(1), 600. https://doi.org/10.1186/s13287-025-04699-3

Iaquinta, M. R., Mazzoni, E., Bononi, I., Rotondo, J. C., Mazziotta, C., Montesi, M., Sprio, S., Tampieri, A., Tognon, M., & Martini, F. (2019). Adult stem cells for bone regeneration and repair. Frontiers in Cell and Developmental Biology, 7, 268. https://doi.org/10.3389/fcell.2019.00268

Kangari, P., Talaei-Khozani, T., Razeghian-Jahromi, I., & Razmkhah, M. (2020). Mesenchymal stem cells: Amazing remedies for bone and cartilage defects. Stem Cell Research & Therapy, 11(1), 492. https://doi.org/10.1186/s13287-020-02001-1

Kitahara, T., Tateiwa, D., Hirai, H., Ikuta, M., Furuichi, T., Bun, M., Ukon, Y., Kanie, Y., Furuya, M., Fujimori, T., Okada, S., & Kaito, T. (2024). rhBMP-2-loaded hydroxyapatite/beta-tricalcium phosphate microsphere/hydrogel composite promotes bone regeneration in a novel rat femoral

nonunion model. Frontiers in Bioengineering and Biotechnology, 12, 1461260. https://doi.org/10.3389/fbioe.2024.1461260

Knight, M., & Hankenson, K. D. (2013). Mesenchymal stem cells in bone regeneration. Advances in Wound Care, 2(6), 306–316. https://doi.org/10.1089/wound.2012.0420

Kushioka, J., Chow, S. K., Toya, M., Tsubosaka, M., Shen, H., Gao, Q., Li, X., Zhang, N., & Goodman, S. B. (2023). Bone regeneration in inflammation with aging and cell-based immunomodulatory therapy. Inflammation and Regeneration, 43(1), 23. https://doi.org/10.1186/s41232-023-00279-1

Lin, T., Pajarinen, J., Nabeshima, A., Lu, L., Nathan, K., Jämsen, E., Yao, Z., & Goodman, S. B. (2017). Preconditioning of murine mesenchymal stem cells synergistically enhanced immunomodulation and osteogenesis. Stem Cell Research & Therapy, 8(1), 277. https://doi.org/10.1186/s13287-017-0730-z

Loi, F., Córdova, L. A., Pajarinen, J., Lin, T., Yao, Z., & Goodman, S. B. (2016). Inflammation, fracture and bone repair. Bone, 86, 119–130. https://doi.org/10.1016/j.bone.2016.02.020

Lopes, D., Martins-Cruz, C., Oliveira, M. B., & Mano, J. F. (2018). Bone physiology as inspiration for tissue regenerative therapies. Biomaterials, 185, 240–275. https://doi.org/10.1016/j.biomaterials.2018.09.028

Lou, T., Chen, K., Luo, Q., Liu, C., Yuan, Y., & Fan, C. (2022). Periosteum-inspired in situ CaP generated nanocomposite hydrogels with strong bone adhesion and superior stretchability for accelerated distraction osteogenesis. Biomaterials Research, 26(1), 78. https://doi.org/10.1186/s40824-022-00330-1

Maldonado, V., Patel, N., Smith, E. E., Barnes, C. L., Gustafson, M. P., Rao, R. R., & Samsonraj, R. M. (2023). Clinical utility of mesenchymal stem/stromal cells in regenerative medicine and cellular therapy. Journal of Biological Engineering, 17(1), 42. https://doi.org/10.1186/s13036-023-00361-9

Maruyama, M., Rhee, C., Utsunomiya, T., Zhang, N., Ueno, M., Yao, Z., & Goodman, S. B. (2020). Modulation of the inflammatory response and bone healing. Frontiers in Endocrinology, 11, 386. https://doi.org/10.3389/fendo.2020.00386

Mededovic, M. (2024). Development of gene delivery coating for orthopedic implants: Enhanced gap junction communication in MSCs accelerates ischemic bone fracture healing [Doctoral dissertation, University of Michigan]. Deep Blue Repository. https://doi.org/10.7302/23983

Mi, B., Xiong, Y., Zha, K., Cao, F., Zhou, W., Abbaszadeh, S., Ouyang, L., Liao, Y., Hu, W., Dai, G., Zhao, Z., Feng, Q., Shahbazi, M., & Liu, G. (2023). Immune homeostasis modulation by hydrogel-guided delivery systems: A tool for accelerated bone regeneration. Biomaterials Science, 11(18), 6035–6050. https://doi.org/10.1039/d3bm00544e

Miletić, M., Puač, N., Škoro, N., Brković, B., Andrić, M., Prokić, B., Danilović, V., Milutinović-Smiljanić, S., Ajtić, O. M., & Mojsilović, S. (2022). Assessment of the potential of cold plasma-pretreated beta-tricalcium phosphate in combination with periodontal ligament stem cells to enhance bone regeneration in vivo. Research Square. https://doi.org/10.21203/rs.3.rs-2206274/v1

Muire, P. J., Mangum, L. H., & Wenke, J. C. (2020). Time course of immune response and immunomodulation during normal and delayed healing of musculoskeletal wounds. Frontiers in Immunology, 11, 1056. https://doi.org/10.3389/fimmu.2020.01056

Netea, P. D. M. G. (2024). Proceedings of the Inter-Disciplinary Conclave (IDC-2023) during the NCRM NICHE 2023. Journal of Stem Cells and Regenerative Medicine, 19(2), 1–89. https://doi.org/10.46582/jsrm.1902009

Ni, F., Chang, L., Peng, Y., Li, D., Wu, D., Li, K., Zhang, X., Jiang, X., Shao, Z., Chen, Y., & Wang, H. (2025). Nano MgO loaded thermosensitive HPCH@HA hydrogel accelerates in situ bone repair through osteoimmunomodulation while enhancing angiogenesis and osteogenesis. Bioactive Materials, 54, 248–266. https://doi.org/10.1016/j.bioactmat.2025.08.007

Oryan, A. (2016). Mesenchymal stem cells and immunomodulation: Implications in bone tissue engineering. International Clinical Pathology Journal, 2(6), 00060. https://doi.org/10.15406/icpjl.2016.02.00060

Pajarinen, J., Lin, T., Gibon, E., Kohno, Y., Maruyama, M., Nathan, K., Lu, L., Yao, Z., & Goodman, S. B. (2018). Mesenchymal stem cell-macrophage crosstalk and bone healing. Biomaterials, 196, 80–89. https://doi.org/10.1016/j.biomaterials.2017.12.025

Sanghani-Kerai, A., McCreary, D., Lancashire, H. T., Osagie-Clouard, L., Coathup, M., & Blunn, G. (2018). Stem cell interventions for bone healing: Fractures and osteoporosis. Current Stem Cell Research & Therapy, 13(5), 369–381. https://doi.org/10.2174/1574888x13666180410160511

Schlundt, C., Schell, H., Goodman, S. B., Vunjak-Novakovic, G., Duda, G. N., & Schmidt-Bleek, K. (2015). Immune modulation as a therapeutic strategy in bone regeneration. Journal of Experimental Orthopaedics, 2(1), 1. https://doi.org/10.1186/s40634-014-0017-6

Smernoff, N. (2024). Mesenchymal stromal cells and their uses in bio-regenerative therapies for bone and cartilage: A review. Open Journal of Regenerative Medicine, 13(1), 1–24. https://doi.org/10.4236/ojrm.2024.131001

Utsunomiya, T., Zhang, N., Lin, T., Kohno, Y., Ueno, M., Maruyama, M., Rhee, C., Huang, E., Yao, Z., & Goodman, S. B. (2021). Different effects of intramedullary injection of mesenchymal stem cells during the acute vs. chronic inflammatory phase on bone healing in the murine continuous polyethylene particle infusion model. Frontiers in Cell and Developmental Biology, 9, 631063. https://doi.org/10.3389/fcell.2021.631063

Watson, L., Elliman, S. J., & Coleman, C. M. (2014). From isolation to implantation: A concise review of mesenchymal stem cell therapy in bone fracture repair. Stem Cell Research & Therapy, 5(2), 51. https://doi.org/10.1186/scrt439

Wu, M., Liu, H., Zhu, Y., Wu, P., Chen, Y., Deng, Z., Zhu, X., & Cai, L. (2024). Bioinspired soft-hard combined system with mild photothermal therapeutic activity promotes diabetic bone defect healing via synergetic effects of immune activation and angiogenesis. Theranostics, 14(10), 4014–4034. https://doi.org/10.7150/thno.97335

Wu, P., Shen, L., Liu, H., Zou, X., Zhao, J., Huang, Y., Zhu, Y., Li, Z., Xu, C., Luo, L., Luo, Z., Wu, M., Cai, L., Li, X., & Wang, Z. (2023). The marriage of immunomodulatory, angiogenic, and osteogenic capabilities in a piezoelectric hydrogel tissue engineering scaffold for military medicine. Military Medical Research, 10(1), 35. https://doi.org/10.1186/s40779-023-00469-5

Yang, S., Zhou, Y., Yu, X., Fu, Z., Zhao, C., Hu, Y., Lin, K., & Xu, Y. (2024). A xonotlite nanofiber bioactive 3D-printed hydrogel scaffold based on osteo-

/angiogenesis and osteoimmune microenvironment remodeling accelerates vascularized bone regeneration. Journal of Nanobiotechnology, 22(1), 392. https://doi.org/10.1186/s12951-024-02323-9

Yang, T., Fang, Z.-L., Zhang, J., & Zheng, S. (2025). Physical cues in biomaterials modulate macrophage polarization for bone regeneration: A review. Frontiers in Bioengineering and Biotechnology, 13, 1640560. https://doi.org/10.3389/fbioe.2025.1640560

Yao, W., Lay, Y.-A. E., Kot, A., Liu, R., Zhang, H., Chen, H., Lam, K. S., & Lane, N. E. (2016). Improved mobilization of exogenous mesenchymal stem cells to bone for fracture healing and sex difference. Stem Cells, 34(10), 2587–2600. https://doi.org/10.1002/stem.2433

Zhang, R., Tan, S. F., Li, Y., Wu, J., & Zhang, C. (2025). From macrophage polarization to clinical translation: Immunomodulatory hydrogels for infection-associated bone regeneration. Frontiers in Cell and Developmental Biology, 13, 1684357. https://doi.org/10.3389/fcell.2025.1684357

Zhang, S., Lü, C., Zheng, S., & Hong, G. (2024). Hydrogel loaded with bone marrow stromal cell-derived exosomes promotes bone regeneration by inhibiting inflammatory responses and angiogenesis. World Journal of Stem Cells, 16(5), 499–518. https://doi.org/10.4252/wjsc.v16.i5.499

Zhang, Y., Fan, M., Zhang, Y., Zhang, Y., & Zhang, Y. (2024). Revolutionizing bone defect healing: The power of mesenchymal stem cells as seeds. Frontiers in Bioengineering and Biotechnology, 12, 1421674. https://doi.org/10.3389/fbioe.2024.1421674